

Improved Flux Formulations for Unsteady Low Mach Number Flows

A. Hosangadi^{*}, J. Sachdev^{*} and V. Sankaran^{**}
Corresponding author: hosangad@craft-tech.com

* Combustion Research and Flow Technology, USA
** Air Force Research Laboratory, USA.

Abstract: Preconditioning techniques that are used to alleviate numerical stiffness due to low Mach numbers in steady flows have typically not performed well for unsteady low Mach problems because the preconditioning scaling requirements for preserving discrete accuracy in time-accurate flows are very different from those for steady flows. Specifically, distinct scalings are necessary for the velocity and pressure fields under the low-Mach, high-Strouhal conditions characteristic of acoustic wave problems. In this article, a unified flux formulation is presented where the optimal scaling required for spatial accuracy is maintained over a broad range of flow conditions. Both upwind flux-difference and AUSM-type schemes are investigated and, in both cases, the judicious use of “steady” and “unsteady” preconditioning scalings in the flux formulation is shown to be critical for preserving accuracy. Low Mach number vortex propagation and acoustic problems are used to demonstrate the strengths of the formulation. These studies show that the AUSM family generally performs better than the blended flux-difference schemes especially in terms of vortex shape preservation.

Keywords: Low Mach Number Preconditioning, Unsteady Flow.

1 Introduction

Accurate and efficient modeling of unsteady low Mach number flows continues to be a challenging problem since it requires the resolution of disparate time scales. Unsteady effects may arise from a combination of hydrodynamic effects in which pressure fluctuations are generated by unsteady velocity fluctuations, and acoustic effects where pressure fluctuations correlate with density fluctuations even if the mean Mach number is very low. Examples in the former category would include vortex propagation problems and bluff body shedding, while examples of the latter include both aeroacoustic problems as well as acoustic wave propagation in internal flows among others. Many practical applications including rotorcraft flows, jets and shear layers include a combination of both acoustic and hydrodynamic effects. Furthermore these effects may be localized with the flow characteristics varying in the domain. Typically the near-field may exhibit non-linear coupling between the different modes of unsteadiness, while the far-field may show a separation of vortex propagation and acoustic scales more typical of low Mach number flows. Therefore, it is important that an algorithm designed for unsteady low Mach number flows function efficiently over a broad range of flow conditions and accurately resolve the inherent stiffness of the system.

Accurate unsteady simulations of these complex low Mach number flows pose difficulties for time-marching algorithms. Preconditioning techniques that are traditionally used to alleviate numerical stiffness work well for steady state simulations but have problems with both efficiency and accuracy

for unsteady computations. One crucial factor arises from the conflicting requirements placed on the flux procedure: the preconditioning scaling that is optimal for accuracy of momentum and energy transport is different from that needed for accuracy of the acoustic (pressure) waves under the low-Mach, high-Strouhal conditions characteristic of acoustic problems. The goal of the current effort is the development of a unified numerical flux procedure where the optimal scalings required for spatial accuracy of all fields are preserved over a wide range of flow conditions. A related aspect of this work is the design of preconditioning procedures to preserve optimal convergence efficiency as well without impacting the underlying accuracy of the discrete formulation.

The development of preconditioning algorithms has been a very active area of research in the literature and many flavors of flux procedures have been developed. These schemes can be broadly classified into two families based on their general characteristics for low Mach number flows: 1) flux-difference/matrix-dissipation preconditioning algorithms [1]-[4] and 2) the AUSM family of flux-splitting schemes [5]-[8]. Both sets of algorithms have been applied with success to steady low Mach number flows by recognizing that the standard flux formulations for higher Mach numbers generate too little dissipation in the pressure field and too much dissipation in the velocity field. By reformulating the equations by introducing a preconditioning matrix (as in the flux-difference schemes) or by modifying the flux formulation using a preconditioning scaling term (as in the AUSM+up schemes), the stiff acoustic speeds are scaled to the local convective velocity and good solution convergence and accuracy is obtained for “all speeds”.

For unsteady flows at low Mach numbers and high Strouhal numbers (needed to resolve acoustic waves), the steady preconditioning scaling that effectively filters the acoustics from the solution becomes far too dissipative for the acoustic/pressure field. More generalized definitions of the preconditioning parameter have been proposed that take the local Strouhal number into account [9]. Here, the preconditioning parameter reverts back to its non-preconditioned value as acoustic effects become dominant thus restoring the ability to accurately model acoustic propagation with good convergence. However, a key drawback of this unsteady preconditioning scaling, especially for the flux-difference procedures, is that the formulation becomes inaccurate for the velocity and temperature fields which are still governed by the convective fluid time scales and not the acoustic time scales. Therefore, solutions to unsteady low Mach number problems may show a disconcerting disconnect between the accuracy requirements of the velocity and the acoustic fields [1].

In an effort to improve on this behavior, Sankaran and Merkle reformulated the flux-difference scheme with features akin to the AUSM schemes [9]. Here, the eigenvalue matrix used for spatial flux dissipation was altered such that the eigenvalue associated with pressure equation corresponded to the acoustic wave from the unsteady preconditioned system whereas all the other equations use the convective velocity. While accurate results with unsteady preconditioning are reported for both acoustic and vortex propagation problem, the concern with this formulation is that the spatial dissipation does not reduce to the “steady” preconditioning form if unsteady effects are not dominant. To avoid this discrepancy for steady calculations, Potsdam et al. [1] formulated a “blended” procedure by defining selection matrices that use the flux from the “unsteady” preconditioning matrix for the continuity equation (or the pressure field) and the flux from “steady” preconditioning for the momentum and energy equations (or the velocity and temperature fields) [1]. In the limit of steady flow, the “unsteady” preconditioning parameter for the continuity equation automatically reverts back to the steady preconditioning parameter and the overall steady preconditioning formulation is recovered.

The second class of numerical flux procedures, the AUSM family of flux-split schemes has also been extended to low Mach number flows [5]-[8]. A key characteristic of AUSM schemes is that the convective flux is separated from the pressure flux; both flux terms are computed independently as scalar formulations thus making it possible to independently tailor the dissipation for hydrodynamic and acoustic unsteadiness. The convective flux terms have essentially a upwinded form with additional dissipation at low Mach numbers; Liou demonstrates excellent results for steady low Mach number flows in the AUSM+up formulation, wherein the “u” and “p” refer to velocity and pressure dissipation terms that have been introduced into the basic AUSM+. Specifically, the magnitude of the

pressure dissipation term is controlled by the introduction of the steady preconditioning scaling in order to obtain uniform accuracy of this term at all Mach numbers [5]. Shima and Kitamura [7],[8] have proposed a variant to the AUSM scheme, referred to as the SLAU scheme (Simple Low Dissipation AUSM), which has been applied primarily to unsteady flows. Interestingly, this scheme does not involve any explicit modifications for low Mach numbers, but as we will later show, this scheme is naturally formulated for unsteady low-Mach acoustic problems.

The focus of this paper is to present a more generalized preconditioning framework based on an unsteady Mach number parameter which ensures that the flux formulation is accurate and efficient for both hydrodynamic and acoustic instabilities, and reverts to the traditional steady flux form in the limit of steady low Mach number flows. The generalized unsteady preconditioning framework has been adapted for both AUSM and flux-difference schemes. The flux-difference procedures are derived by developing “blended” formulations of the “unsteady” and “steady” preconditioning parameters and are extensions of the work presented by Potsdam et al. [1]. For the AUSM family of schemes, the dissipation parameters for both the mass flux and pressure terms have been modified using the unsteady Mach number parameter. The modified AUSM schemes are referred to as AUSM+up’ and AUSM+u’p’, where the “primes” designate that the pressure and/or velocity dissipation terms are being scaled by the unsteady Mach number. Corresponding modifications are proposed for the SLAU scheme as well. Both the blended flux-difference and the modified AUSM+up formulations are tested on a range of unit problems encompassing both hydrodynamic and acoustic instabilities. Solution accuracy and unsteady inner iteration convergence are evaluated for these problems to demonstrate their wide range of applicability.

2 Flux Formulations for Low Mach Number Unsteady Flows

The formulation of a more generalized unsteady preconditioning framework for both flux differenced and AUSM family of schemes is described here. We begin by giving a brief overview of the preconditioned system of equations and steady preconditioning for flux difference schemes in Sections 2.1 and 2.2. The “blended” flux difference formulations for unsteady preconditioning that were developed as part of this effort are described in Section 2.3. The AUSM family of schemes is described in Section II.D and an analysis comparing AUSM+up and SLAU is discussed here. The extensions for AUSM+up’ and AUSM+u’p’ employing the unsteady preconditioning parameter are described in Section 2.5.

2.1 Preconditioned Equation System

The standard conservative form of the equations (with a two-equation turbulence model) may be written as

$$\frac{\partial Q}{\partial t} + \frac{\partial E}{\partial x} + \frac{\partial F}{\partial y} + \frac{\partial G}{\partial z} = S + D_v \quad (1)$$

where $Q = [\rho, \rho u, \rho v, \rho w, e, \rho k, \rho \varepsilon]^T$ represents the vector of conserved variables; E , F and G are the flux vectors; S represents the source terms (if any); and D_v represents the viscous fluxes. For low Mach number flows as density approaches a constant the conservative variables become ineffective for temporal integration. In this flow regime, the primitive variables vector, $Q_v = [p, u, v, w, T, k, \varepsilon]^T$, constitutes a particularly effective choice. Primitive variables replace the density by pressure, thereby avoiding round-off errors, and the total energy by temperature which is more compatible with the thermal diffusion terms and for modeling multi-species flows (as, for example, the combusted exhaust plume from an aircraft engine).

One effective way for expressing a general iterative method is through a dual-time formulation. Upon appending a pseudo-time derivative and a preconditioning matrix, Γ_p , Eqn. (1) takes the form;

$$\Gamma_p \frac{\partial Q_v}{\partial \tau} + \frac{\partial Q}{\partial t} + \frac{\partial E}{\partial x} + \frac{\partial F}{\partial y} + \frac{\partial G}{\partial z} = S + D_v \quad (2)$$

The numerical characteristics of the pseudo-time in this equation are determined by the eigenvalues of the matrix, $[\Gamma_p^{-1}(\partial E / \partial Q_v)]$ which are:

$$\Lambda = \text{diag} \left[\frac{1}{2} \left[\hat{U}(1+R) \pm \sqrt{\hat{U}^2(1-R)^2 + 4c'^2(I_x^2 + I_y^2 + I_z^2)} \right], \hat{U}, \hat{U}, \hat{U}, \hat{U} \right] \quad (3)$$

where R represents the ration of the square of the pseudo-acoustic speed and the physical acoustic speed which can be expressed as the square of the ratio of the physical Mach number to a pseudo-Mach number as

$$R = \frac{(\rho \rho_p h_T + \rho_T(1 - \rho h_p))}{(\rho \rho_p' h_T + \rho_T(1 - \rho h_p))} = \left(\frac{c'}{c} \right)^2 = \left(\frac{M}{M'} \right)^2 \quad (4)$$

This system of equations can be made well-conditioned by choosing ρ_p' to be of order $\rho_p' \approx [O(1/u^2)]$, thereby resulting in a pseudo-sound speed, $c' \approx [O(u)]$. The preconditioning parameter, ρ_p' , can be expressed in terms of the ratio of pseudo-Mach number to physical-Mach number and the ratio of specific heats:

$$\frac{\rho_p'}{\rho_p} = \frac{1}{\gamma} \left(\frac{M'}{M_p} \right)^2 + \frac{\gamma-1}{\gamma} \quad (5)$$

where

$$M_p^2 = \min \left[\max(M_i^2, M_u^2, M_{\min}^2), 1 \right] \quad (6)$$

Here, M_i is the local Mach number, M_{\min} is a user specified cut-off Mach number to preclude difficulties at stagnation points, and M_u is an ‘‘unsteady’’ preconditioning scaling. This unsteady preconditioning term can be related to the global Strouhal number for the problem as:

$$M_u = \frac{L}{\pi c \Delta t} \quad (7)$$

where L is a global length scale and Δt is the time-step. In the following discussions, Eqn. (6) without the unsteady preconditioning scaling is referred to as steady preconditioning formulation, while the full version of Eqn. (6) is called the unsteady preconditioning formulation.

2.2 Flux-Difference Algorithm: Roe’s Scheme with Steady or Unsteady Preconditioning

The inviscid flux at cell interfaces is calculated with an approximate Riemann solver given the reconstructed left and right solution states. The flux difference/matrix-dissipation procedure based on Roe’s scheme [11] can be given as:

$$F_m = \frac{1}{2} \left\{ F(Q_v^-, \bar{n}) + F(Q_v^+, \bar{n}) + \Delta F^-(\hat{Q}_v, \bar{n}) + \Delta F^+(\hat{Q}_v, \bar{n}) \right\} \quad (8)$$

where \bar{n} is the area-directed normal of either the cell face or the dual face crossing the edge, Q_v^- and Q_v^+ are the left and right primitive state variables, and \hat{Q}_v denotes the Roe-averaged variables. The flux differences ΔF^- and ΔF^+ are given by:

$$\Delta F^+(\hat{Q}_v, \bar{n}_{oi}) = \frac{1}{2} \left(\hat{\Gamma}_p \hat{R}_p (\hat{\Lambda}_p + |\hat{\Lambda}_p|) \hat{L}_p \right) (Q_v^+ - Q_v^-) \quad (9)$$

$$\Delta F^-(\hat{Q}_v, \bar{n}_{oi}) = \frac{1}{2} \left(\hat{\Gamma}_p \hat{R}_p (\hat{\Lambda}_p - |\hat{\Lambda}_p|) \hat{L}_p \right) (Q_v^+ - Q_v^-) \quad (10)$$

Here Γ_p , R_p , L_p , and Λ_p are the preconditioning matrix, right eigenvector matrix, left eigenvector matrix, and diagonal eigenvalue matrix \hat{Q}_v for the preconditioned system computed with the Roe-averaged variables.

2.3 Flux-Difference Algorithms: Blended Unsteady/Steady Preconditioned Schemes

The standard flux difference formulation shown above (Eqns. (9) and (10)) indicate that the spatial dissipation is intimately tied to the time scaling defined by the preconditioning matrix. Table 1 gives the behavior of the pressure and velocity dissipation terms for both steady low Mach numbers and for unsteady low-Mach, high-Strouhal numbers. In the steady low Mach case, the use of no preconditioning clearly leads to ill-behaved artificial dissipation terms with the pressure dissipation becoming vanishingly small and the velocity dissipation becoming unboundedly large. The use of the steady or inviscid preconditioning in Eqn. (6) clearly alleviates this situation and both the pressure and velocity dissipation terms become the same magnitude as the dominant physical terms in the equations of motion. The situation for unsteady flows in the low-Mach, high-Str limit is more challenging. It can be observed that using just the inviscid preconditioning in the flux formulation leads to increased dissipative errors in the pressure field, while the velocity dissipation is well-behaved. In contrast, when the unsteady preconditioning scaling given in Eqn. (6) is used, the pressure dissipation is well behaved, while the velocity dissipation becomes too large. Thus, no scaling of the standard flux-difference formulation naturally preserves the discretization accuracy in the unsteady case.

Table 1: Normalized scaling of the pressure and velocity dissipation terms in the steady low-Mach limit and the unsteady low-Mach, high-Str limit for different preconditioning scalings in the flux-difference scheme.

Formulation	Steady Low Mach Limit		Unsteady Low-Mach High-Str	
	Pressure	Velocity	Pressure	Velocity
No preconditioning	O(M)	O(1/M)	O(1)	O(1/M)
Steady Preconditioning	O(1)	O(1)	O(1/M)	O(1)
Uns. Preconditioning	O(1)	O(1)	O(1)	O(1/M)
Blended scheme	O(1)	O(1)	O(1)	O(1)

Also shown in Table 1 is the so-called blended formulation which is constructed so that “steady” and “unsteady” preconditioning forms can be used for specific terms in the momentum and energy equations, thereby controlling the pressure and velocity dissipation scaling independently. These formulations are devised by exploiting the form of the algebraic expressions for the spatial dissipation terms. The combination of the spatial dissipation terms in Eqns. (9) and (10) may be written as a matrix, C_p , multiplied by the change in the primary dependent variable vector:

$$\Delta F^+(\hat{Q}_v, \bar{n}_{oi}) + \Delta F^-(\hat{Q}_v, \bar{n}_{oi}) = C_p (Q_v^+ - Q_v^-) \quad (11)$$

where the combined dissipation matrix, C_p , can be written out as

$$C_p = \begin{pmatrix} C_{11} & C_{12} & C_{13} & C_{14} & C_{15} & C_{16} & C_{17} \\ uC_{11} + C'_{21} & uC_{12} + C'_{22} & uC_{13} + C'_{23} & uC_{14} + C'_{24} & uC_{15} + C'_{25} & uC_{16} & uC_{17} \\ vC_{11} + C'_{31} & \dots & \dots & \dots & \dots & \dots & \dots \\ wC_{11} + C'_{41} & \dots & \dots & \dots & \dots & \dots & \dots \\ HC_{11} + C'_{51} & HC_{12} + C'_{52} & HC_{13} + C'_{53} & HC_{14} + C'_{54} & HC_{15} + C'_{55} & HC_{16} & HC_{17} \\ kC_{11} & kC_{12} & kC_{13} & kC_{14} & kC_{15} & kC_{16} & kC_{17} \\ \varepsilon C_{11} & \dots & \dots & \dots & \dots & \dots & \dots \end{pmatrix} \quad (12)$$

The form of this matrix shows that the entries for the scalar transport equations, such as those for the turbulence scalars or species equations for combusting flows, are multiples of the first row (the continuity equation) scaled by the convected property of that equation. Similarly, the entries for the momentum and energy equations contained one term that is a product of the first row multiplied by the pertinent local scalar (e.g., u , H), however, they also include an additive correction term which is a

function of the eigenvalues. Therefore, the form of this matrix suggests “blended” schemes in which steady and unsteady preconditioning can be applied to different parts of this matrix.

One choice of blended scheme is constructed by decomposing the dissipation matrix into two terms as given by

$$\Delta F^+ + \Delta F^- = (C\Phi^T + C'_p)(Q_v^+ - Q_v^-) \quad (13)$$

where the first term is given by the tensor product of two vectors given by $C = (C_{11} \ C_{12} \ C_{13} \ C_{14} \ C_{15} \ C_{16} \ C_{17})$ and $\Phi = (1 \ u \ v \ w \ H \ k \ \varepsilon)$ and the second term is a correction matrix C'_p . This matrix structure suggests a sophisticated blending strategy in which “steady” and “unsteady” preconditioning forms could be used for specific terms in the momentum and energy equations which may be written as:

$$\Delta F^+ + \Delta F^- = (C\Phi^T + C'_p)(Q_v^+ - Q_v^-) \quad (14)$$

Here the $C\Phi^T$ terms use “unsteady” (green notation) while the C'_p terms could use “steady” preconditioning (red notation). This blending scheme is equivalent to having the first row of the C_p matrix with unsteady preconditioning while the other rows will have a combination of steady and unsteady preconditioning terms. The last row of Table 1 shows that such a scaling strategy results in well-behaved pressure and velocity terms in both the steady and unsteady limits.

Other choices of blended schemes are possible, but have been observed to yield similar scaling results and so are not investigated further here. Also, we note that this blended scheme is similar (but not identical) to the scheme proposed by Potsdam et al. [1].

2.4 AUSM Type Algorithms for Preconditioned Systems

Flux-splitting schemes provide an alternative approach to flux difference schemes for calculating the inviscid flux at cell interfaces. These procedures are attractive since they provide a natural means to decouple the dissipation for the momentum and pressure flux thus allowing more flexibility to tailor the dissipation for acoustic and hydrodynamic instabilities in unsteady flows. Prior to describing the extensions to an unsteady preconditioning framework we analyze the differences between the AUSM+up scheme [5] developed by Liou and the SLAU scheme derived from AUSM by Shima and Kitamura [7],[8] specifically for low Mach number flows. These schemes are described below.

The numerical flux for flux-split schemes is given by

$$\tilde{F} = \frac{\dot{m} + |\dot{m}|}{2} \Phi^+ + \frac{\dot{m} - |\dot{m}|}{2} \Phi^- + \tilde{p}\tilde{n} \quad (15)$$

$$\Phi = (1, u, v, w, h_t)^T \quad (16)$$

The unique formulation of the AUSM family schemes is determined by the choice of mass flux function, \dot{m} , and average pressure, \tilde{p} . The mass flux in AUSM+up scheme is given by

$$\dot{m} = \bar{c}M_{1/2} \begin{cases} \rho_L & \text{if } M_{1/2} > 0 \\ \rho_R & \text{otherwise} \end{cases}, \quad (17)$$

$$M_{1/2} = M_{(4)}^+(M_L) + M_{(4)}^-(M_R) - \frac{K_p}{f_a} \max(1 - \sigma \bar{M}^2, 0) \frac{p_R - p_L}{\bar{\rho} \bar{c}^2}$$

Here $M_{(4)}^\pm$ are fourth order polynomials in Mach number. The last term is a dissipation term formulated for low Mach number flows. The f_a term in the denominator increases the dissipation in inverse proportion to the Mach number and is equivalent to a steady preconditioning parameter. It is defined as:

$$f_a = M_o(2 - M_o) \in [0, 1], \quad M_o^2 = \min\left(1, \max\left(\bar{M}^2, M_{\min}^2\right)\right), \quad \bar{M}^2 = \left(u_L^2 + u_R^2\right) / 2\bar{c}^2 \quad (18)$$

Making a low Mach number assumption and dropping higher order terms in Mach number Eqn. (17) can be rewritten as:

$$\dot{m} = \rho^\pm \left\{ \frac{1}{2} (V_n^+ + V_n^-) - \frac{K_p}{f_a} \max(1 - \sigma \bar{M}^2, 0) \frac{P_R - P_L}{\bar{\rho} \bar{c}} \right\} \quad (19)$$

where ρ^\pm is ρ^+ for $M_{1/2}$ greater than zero and ρ^- otherwise.

The pressure flux formulation in the AUSM+up scheme is given by;

$$\tilde{p} = P_{(5)}^+(M_L) p_L + P_{(5)}^-(M_R) p_R - 2K_u P_5^+ P_5^- \bar{\rho} f_a \bar{c} \Delta u \quad (20)$$

Here $P_{(5)}^\pm$ are fifth-order polynomials in Mach number while the last term, which can be summarized as the p_u dissipation term, is a dissipation term that operates at transonic Mach numbers and decreases in value as the Mach number drops. Making a low Mach number assumption and *dropping higher order terms in Mach number* this equation reduces to:

$$\tilde{p} = \frac{1}{2} (p^+ + p^-) + \frac{3}{4} (M^+ p^+ - M^- p^-) - \frac{3}{8} [2M] \bar{\rho} \bar{c} \Delta u \quad (21)$$

where the [2M] factor in the last term comes from the expression for f_a .

For the SLAU scheme given by Shima and Kitamura [7],[8], the mass flux is given directly in the simplified low Mach number form as

$$\dot{m} = \frac{1}{2} \left\{ \rho^+ (V_n^+ + |\bar{V}_n|^+) + \rho^- (V_n^- - |\bar{V}_n|^-) \right\} - \frac{\chi}{2\bar{c}} \Delta p \quad (22)$$

$$\chi = 1 - 2M$$

While the pressure flux for the SLAU formulation is given by

$$\tilde{p} = \frac{(p^+ + p^-)}{2} + \frac{(P_{(5)}^+ - P_{(5)}^-)}{2} (p^+ - p^-) + (1 - \chi) (P_{(5)}^+ + P_{(5)}^- - 1) \frac{(p^+ + p^-)}{2} \quad (23)$$

Making a low Mach number assumption and *dropping higher order terms in Mach number* this equation reduces to:

$$\tilde{p} = \frac{1}{2} (p^+ + p^-) + \frac{3}{8} (M^+ + M^-) (p^+ - p^-) - \frac{3}{8} [2M] \bar{\rho} \bar{c} \Delta u \quad (24)$$

where the [2M] factor in the last term comes from the expression for χ .

Comparing the mass flux dissipation for AUSM+up (Eqn. (19)) and SLAU (Eqn. (22)), it is observed that the primary difference for the two schemes is the dissipation that is added at low Mach numbers for the AUSM+up scheme. In the AUSM+up scheme, the dissipation term for the mass flux (which is a pressure dissipation) has the f_a term in the denominator which increases the dissipation substantially as the Mach number drops and behaves like a steady preconditioning parameter. In contrast, the SLAU formulation does not have this term and exhibits only a weak dependence on Mach number from the χ term in the numerator. Therefore, the SLAU scheme would be inadequate for steady low Mach number problems as seen in Table 2, which shows the behavior of the pressure and velocity dissipation terms for the steady low-Mach and unsteady low-Mach/high-Str limits.

In contrast, the AUSM+up scheme is well-behaved for steady low-Mach problems. Interestingly, in the unsteady acoustic limit, the SLAU scheme (which is similar to the basic AUSM+ scheme) performs well, while the AUSM+up scheme introduces too much damping in the acoustic/pressure field. To obtain uniform accuracy under both steady and unsteady limits, we consider in the following section the extensions of the unsteady preconditioning to the AUSM family of schemes.

Table 2: Normalized scaling of the pressure and velocity dissipation terms in the steady low-Mach limit and the unsteady low-Mach, high-Str limit for different preconditioning scalings in the AUSM family of schemes.

Formulation	Steady Low Mach Limit		Unsteady Low-Mach High-Str Limit	
	Pressure	Velocity	Pressure	Velocity
SLAU	O(M)	O(1)	O(1)	O(1)
AUSM+up	O(1)	O(1)	O(1/M)	O(1)
AUSM+up'	O(1)	O(1)	O(1)	O(1)
AUSM+u'p'	O(1)	O(1)	O(1)	O(1/M)

2.5 Extensions of Unsteady Preconditioning Framework to AUSM schemes

As our analysis in the previous section indicates the standard AUSM+up scheme is optimized for steady low Mach number problems. A more general unified formulation that automatically selects the appropriate dissipation level is presented here by formulating the mass flux dissipation in terms of an unsteady Mach number scale. This modified scheme is referred to AUSM+up'; where the pressure prime indicates that the pressure dissipation is scaled by the unsteady Mach number. The dissipation for the mass flux term in the AUSM+up' scheme is generalized by modifying the definition of Mach number used to define the f_a term in Eqn. (18) by including an unsteady preconditioning scale as follows:

$$M_o^2 = \min\left(1, \max\left(\bar{M}^2, M_{\min}^2, M_u^2\right)\right) \quad (25)$$

We note that in the most general configuration the M_u scale can be defined both as a global parameter and as local factor that is computed on the local flow physics. For simpler problems a global parameter might suffice but for more complex physics where the characteristics may vary (e.g. high frequency in the near field of a turbulent jet and low frequency in the far-field) the ability for the numerical formulation to select the automatically select the unsteady scale is crucial. We note that reducing the dissipation for the mass flux term for unsteady acoustic flows has been suggested both by Liou [5] and Vigneron *et al.* [6] however Eqn. (25) provides a means for the numerical formulation to self-select the appropriate dissipation level. Table 2 confirms that the resulting scheme is indeed well-behaved in both the steady and unsteady limits of interest.

An additional modification involves changing the pressure dissipation term by adding additional dissipation for low Mach number acoustic problems using the unsteady Mach number parameter. These modifications lead to the AUSM+u'p' scheme where the primes indicate that both pressure and velocity dissipation terms are scaled by the Mach number parameter. The definition of Mach number M_o using the unsteady Mach number scale M_u as shown above in Eqn. (25) also affects the pressure dissipation term in Eqn. (20) as shown below:

$$\begin{aligned} f_a &\approx 0 \text{ when } M_u \approx 0 \text{ for steady low Mach number flows} \\ f_a &\approx 1 \text{ when } M_u \approx 1 \text{ for unsteady low Mach number flows} \end{aligned} \quad (26)$$

In particular, for steady flows no additional dissipation results but for unsteady acoustic low Mach number flows substantial dissipation is added to the pressure flux. Table 2 shows that such a formulation adversely impacts solution accuracy in the velocity field for unsteady acoustic problems. Thus, the AUSM+up' formulation appears to be the ideal choice of scheme for a wide range of steady and unsteady flow conditions with the exception of a narrow class of acoustic propagation problems where the AUSM+u'p' was required (see discussion in Section 3.4). We further note that the dissipation flux modifications in AUSM+up, AUSM+up' and AUSM+u'p' can be implemented in the context of the SLAU scheme as well with similar scaling behaviors of the associated dissipation terms.

3 Evaluation of the Low Mach Number Formulations

The low Mach number formulations described in the previous section were evaluated with several test problems involving hydrodynamic and acoustic unsteadiness. These calculations were performed with the CRUNCH CFD[®] code, developed at CRAFT Tech [12]-[15]. The candidate flux formulations for unsteady low Mach number flows will be tested out rigorously for the following three test cases that include both hydrodynamic and acoustic instabilities: 1) Unsteady inviscid Lamb vortex problem (hydrodynamic instability), 2) Unsteady inviscid flow in a pipe with fluctuating back pressure (mixed acoustic and hydrodynamic instability), and 3) Shock tube with small pressure difference (pure acoustic problem). We note that both the “blended” flux difference and AUSM type schemes have to be run with inconsistent LHS and RHS discretization since these formulations are unstable when a consistent LHS is used. For the results presented here we employ the standard preconditioned Roe flux differenced procedure on the LHS with unsteady preconditioning and dual time stepping at each time step. Prior to discussing the unsteady test cases, a steady low Mach number test case is presented to compare the Roe flux differenced procedure with the SLAU scheme; as discussed earlier the dissipation in the original SLAU scheme is shown to be appropriate only for unsteady flows and this constraint is demonstrated by computing a steady flow-field.

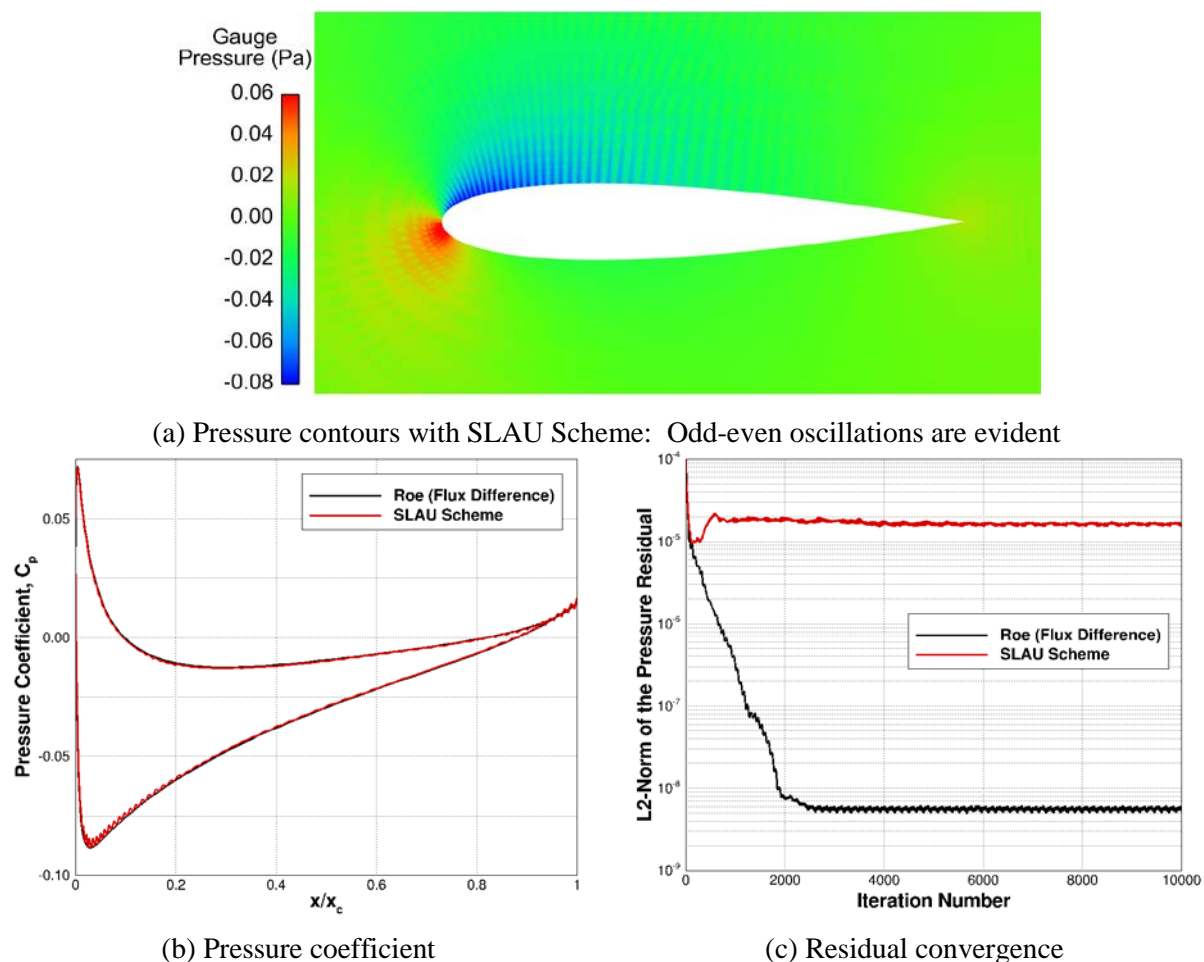


Figure 1. Solution for a steady flow over a NACA0015 airfoil at a freestream Mach number of 0.001 and an angle of attach of 4° as computed with the SLAU scheme and a Roe flux differenced scheme with steady preconditioning.

3.1 Steady Flow over a NACA0015 Airfoil

Steady state calculations were performed for a NACA0015 airfoil, at a freestream Mach number of 0.001, Reynolds number of $1.95E+06$, and an angle-of-attack of 4° using a Roe flux differences procedure with steady preconditioning and the SLAU scheme. The higher order solution and convergence is shown Figure 1 for both schemes. For the SLAU scheme it is noted that the solution shows oscillations with odd-even coupling that is reflected in the surface pressure coefficient. Moreover, the corresponding convergence shown in Figure 1(c) indicates that the SLAU solution does not converge in contrast to the solution with flux difference procedure with steady preconditioning. The numerical instability for the SLAU was verified to result from the low freestream Mach numbers; the odd-even oscillations were not evident when the Mach number was increased to 0.1 (results not shown). Therefore, it was concluded that the mass flux dissipation in Eqn. (22) for SLAU scheme was unable to provide accurate solutions for steady low Mach number flows as expected.

The dissipation term for SLAU was subsequently modified by adding the form of the dissipation from the AUSM+up formulation (Eqn. (19)). Therefore, for steady low Mach number problems substantial dissipation (resulting from the f_a term in the denominator of Eqn. (19) is added to the mass flux term, leading to what we refer to as the SLAU+p scheme. The solution for the NACA0015 airfoil with the modified dissipation term is shown in Figure 2. The flow contours and pressure coefficient are now smooth and the convergence was found to be independent of the Mach number. Therefore, this confirms our premise discussed earlier that the SLAU scheme corresponds to the standard AUSM+ formulation and requires modifications in the steady limit (i.e., the SLAU+p scheme) for low Mach number flows.

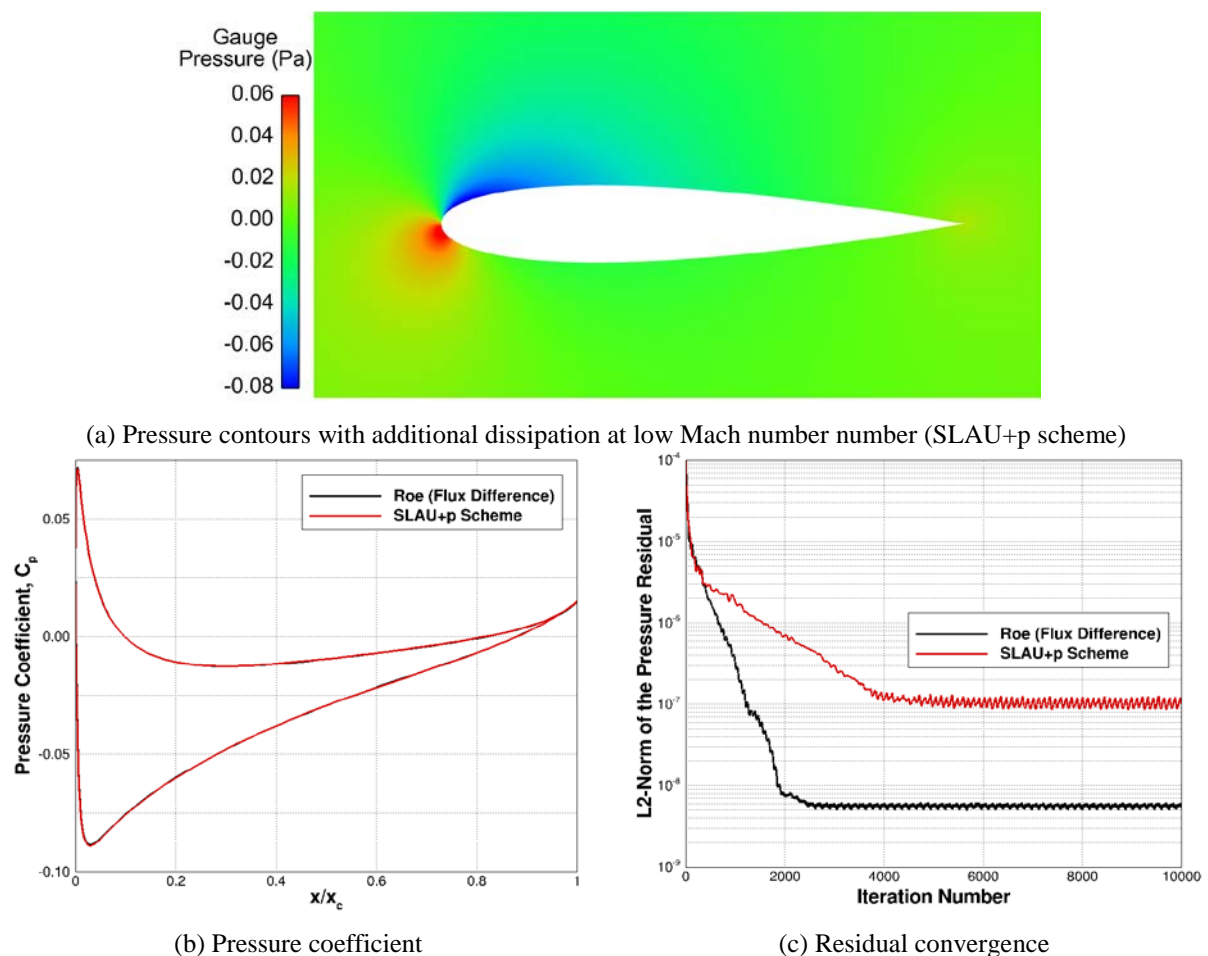


Figure 2. Solution for a steady flow over a NACA0015 airfoil at a freestream Mach number of 0.001 and an angle of attach of 4° as computed with the SLAU+p scheme.

3.2 Vortex Propagation Problem

The propagation of an unsteady convecting inviscid Lamb vortex was used to assess the effectiveness of the flux formulations discussed above for the hydrodynamic class of problems. The velocity distribution in polar coordinates for the Lamb vortex is given by

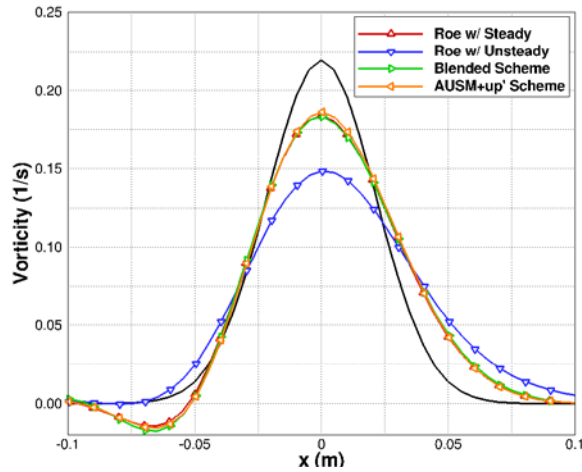
$$V_r = 0 \quad V_\theta = \Gamma \left(\frac{1 - e^{-r^2/\phi^2}}{r} \right) \quad (27)$$

where Γ and ϕ are the vortex strength and characteristic radius of the vortex and were set to $0.1M_\infty$ and 0.03, respectively. Simulations are presented here for a freestream Mach number of 0.001 were computed on a uniform Cartesian grid with a spacing of 0.005. The vortex solution is presented after the vortex has travelled a distance equal to 0.4 on this uniform mesh. The unsteady Mach number scale was specified as done by Potsdam et al. in Ref. [1].

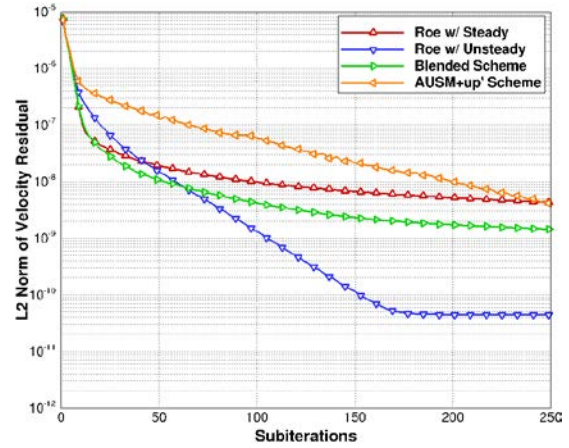
$$M_u = \frac{L(M_\infty)}{\pi(\Delta x)(CFL_u)} \quad (28)$$

For a baseline value of $CFL_u = 1$ this translates to an unsteady Mach number of 2.55E-02. For very small time steps (e.g., $CFL_u = 0.001$) the unsteady Mach number becomes 1 and the dissipation levels are representative of unsteady preconditioning. Results are presented for the baseline time-step dictated by $CFL_u = 1$ and an extremely small time-step given by $CFL_u = 0.001$. Two-hundred and fifty inner iterations were used for all cases. Both the blended flux difference scheme and the AUSM+up' scheme are compared with benchmark values of Roe flux differenced scheme using steady and unsteady preconditioning.

The vortex solution and inner iteration convergence are shown for the baseline time step of $CFL_u = 1$ in Figure 3 for the different schemes. The exact vorticity profile is given by the black line in Figure 3(a). The red and blue lines correspond to the standard flux-difference scheme with steady and unsteady preconditioning, respectively. The result computed with a blended flux formulation is given by the green line whereas the orange line gives the profile computed with the AUSM+up' scheme. The vorticity profiles show that the flux difference scheme with steady preconditioning, the blended flux difference scheme, and the AUSM+up' collapse to essentially the same solution. The solution computed using the flux difference scheme with unsteady preconditioning has poor accuracy compared to the other schemes, however, the convergence plots shows that it has the best rate of convergence indicating optimal time scaling for convergence. Rectification of this inconsistency between solution accuracy and convergence was one of the primary goals at the outset of this research. The convergence for the blended scheme is slightly better than the flux difference scheme with steady preconditioning. The convergence for the AUSM+up' scheme is worse than the blended scheme which is likely due to the increased inconsistency of the left-hand side and right-hand side flux formulations, however, the solution was just as accurate as the blended and pure steady preconditioning schemes.



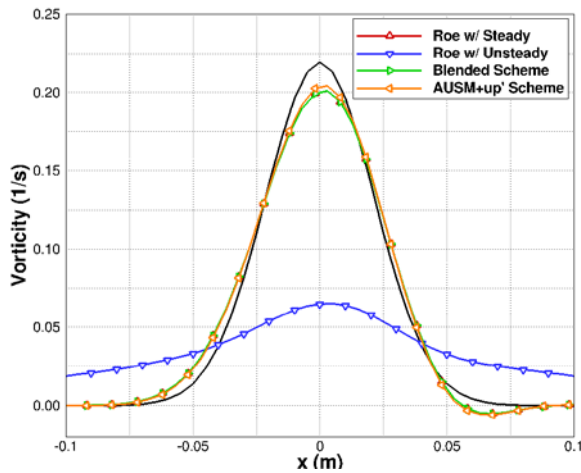
(a) Vorticity profile



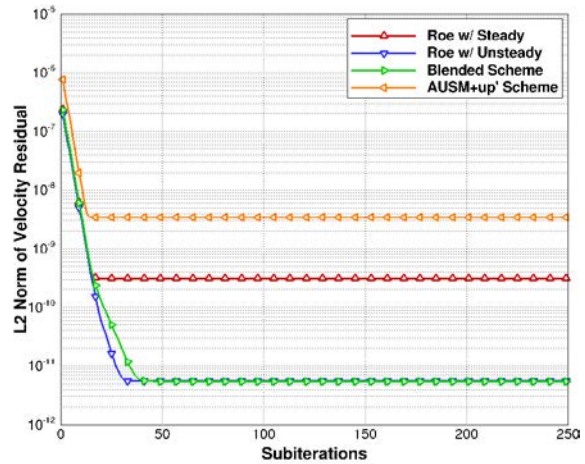
(b) Inner iteration convergence

Figure 3. Vortex solution accuracy and convergence a time-step of $CFL_u = 1$.

To further confirm the insensitivity of the solution accuracy to the unsteady preconditioning parameter, the time-step was reduced to $CFL_u = 0.001$ which goes to the limit of unsteady preconditioning for the blended and AUSM+up' schemes. The vorticity profiles and inner iteration convergence are plotted in Figure 4. At this much smaller time step, the steady preconditioning case and AUSM+up' show essentially flat convergence while the baseline unsteady preconditioning and blended scheme show rapid convergence. From Figure 4(a), it is observed that the accuracy for the baseline unsteady preconditioning scheme deteriorates very dramatically while the blended scheme continues to provide an accurate vorticity profile. Despite the very poor convergence, the AUSM+up' scheme and the baseline scheme with steady preconditioning give as accurate a profile as the blended flux formulation.



(a) Vorticity profile



(b) Inner iteration convergence

Figure 4. Vortex solution accuracy and convergence for a time-step of $CFL_u = 0.001$.

Thus far the predicted vorticity field was considered as the metric for evaluating the solution accuracy. However, while the pressure variations may be very small, its gradient should correspond to the swirl velocity in the vortex. Therefore, it is instructive to evaluate the resulting pressure contours for the difference flux procedures. The vorticity and pressure contours for the various schemes are plotted in Figure 5 and Figure 6, respectively. The flux difference scheme with steady preconditioning gives accurate results for the vorticity field as seen in Figure 5(a), however, the pressure field in Figure 6(a) is very inaccurate. This is not unexpected since the steady preconditioning gives the correct scale for the velocity equation but provides an incorrect scale for the acoustic eigenvalues. The flux difference scheme with unsteady preconditioning gives poor solutions

for both the vorticity and pressure fields in Figure 5(b) and Figure 6(b) due to large dissipation in the velocity equation.

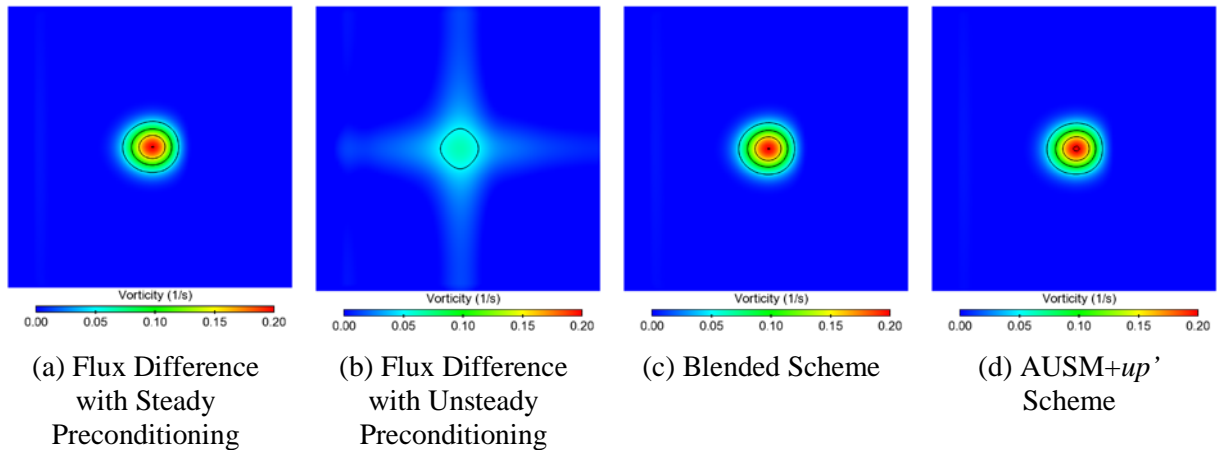


Figure 5: Vorticity field for various flux schemes for a time step of $CFL_u=0.001$.

The blended flux difference scheme gives the correct solution for both the vorticity and pressure field as shown in Figure 5(c) and Figure 6(c), since they use different preconditioning scales for the two variables: unsteady for the pressure wave and steady for the velocity field. However, there appears to be one notable discrepancy in that the pressure field is not circular to match the vortex but is instead distorted to be a rhombus. The cause of this distortion is not fully understood but may be due to the difference in magnitude for the cross-dissipation terms involving the velocity components and the pressure field (e.g., $\Delta u \Delta p$ versus $\Delta v \Delta p$).

The vorticity and pressure fields computed using the modified AUSM+up' scheme can be seen in Figure 5(d) and Figure 6(d). Accurate solutions are realized for both the velocity and pressure fields. In particular, the pressure field does not show the distortion that was evident from the blended scheme results. Moreover, the circular contours in the pressure field accurately match the contours of the velocity field. The blended flux-difference and the AUSM+up' schemes both show odd-even oscillations in the pressure field. The source of this instability is not clear but may be related to the inconsistency between the schemes used for the flux for the implicit and explicit sides.

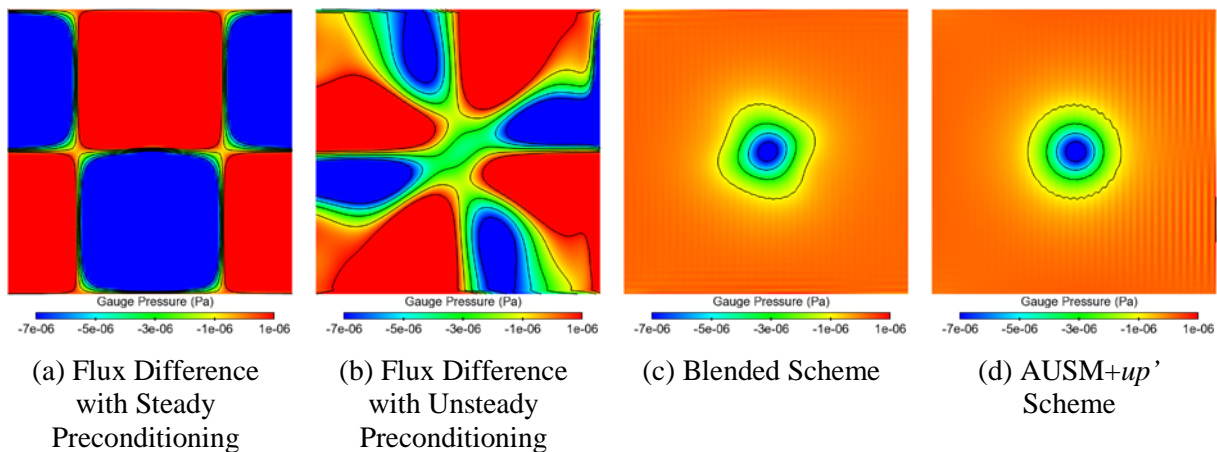


Figure 6: Gauge pressure field for various flux schemes for a time step of $CFL_u=.001$.

In summary, both the blended flux difference and the AUSM+up' schemes are able to provide accurate solutions of the vorticity field and are insensitive to the time step. Both schemes are a substantial improvement over previous baseline flux difference procedures that showed inconsistency between convergence and accuracy with the solution accuracy in particular deteriorating rapidly with unsteady preconditioning. An evaluation of the pressure contours revealed that both the blended flux

difference and the AUSM+up' schemes were able to provide the correct pressure depression in the vortex. However, the solutions for the blended flux difference scheme show a distortion of the pressure field shape. In contrast, the pressure field computed using the AUSM+up' scheme maintained the circular pressure field. The only drawback of the AUSM+up' formulation appears to be less than ideal convergence at small time steps and this is probably related to the inconsistent discretizations on the LHS and RHS. This is potentially an area requiring improvement in terms of efficiency of the procedure.

3.3 Simulations of Flow in a Tube with Oscillating Back Pressure

The next test problem investigated was inviscid flow in a 1-D tube where the back pressure was fluctuated and the inlet pressure was held constant as given by

$$\begin{aligned} P_{x=L} &= P_b(1 + \varepsilon \sin wt) \\ P_{x=0}^o &= \text{constant} \end{aligned} \quad (29)$$

The analytical solution for this scenario is given below:

$$\begin{aligned} u'(t) &= -\left(\frac{\varepsilon}{\rho_L u_0^2}\right)\left(\frac{u_0}{1+\Omega^2}\right)\left[\sin wt - \Omega \cos wt + \Omega e^{\frac{-u_0 t}{L}}\right], \\ P'(x,t) &= \left[\varepsilon \sin wt + \rho u_0 u'\right]\frac{x}{L} - \rho u_0 u', \quad \Omega = \frac{wL}{u_0}, \text{Phase lag } \phi = \tan^{-1}(\Omega) \end{aligned} \quad (30)$$

The velocity field is uniform in space but fluctuates in time, while the pressure field has a linear slope spatially from the inlet to the exit while also fluctuating in time. The key parameter of interest here is the Strouhal number Ω ; as Ω increases the unsteady time scales become dominant and the baseline flux difference procedures provide inaccurate solutions that vary with the preconditioning parameter. Therefore, this problem would be a good test for the validity of both the blended flux difference and the modified AUSM+up' schemes. The objective is to be able to get an accurate solution independent of the preconditioning parameter and frequency.

In the present calculations, the mean Mach number in the tube was specified to be 0.001 and a 5 percent fluctuation amplitude was applied at the exit with 100 inner iterations for the dual time iteration. The frequency and the time step were varied over a broad range to test the robustness and accuracy of the flux procedures over a broad range of conditions. The steady preconditioning Mach number cut-off was specified as 0.001 while the unsteady Mach number scale was set to 1.0. The time step was specified as $2\pi/(PPW \Omega)$ where PPW denotes the points per time period.

For the benign scenario where the fluctuation frequency is low, $\Omega = 1$, and the time-step is large with 10 points per time period, the baseline flux difference scheme with steady and unsteady preconditioning, the blended flux difference scheme, and the AUSM+up' scheme all produced pressure and velocity profiles that matched the exact solution. Essentially in this case the flow behaves like a quasi-steady problem with the time variation being a series of steady variations. The convergence history shows very little difference between steady and unsteady preconditioning for the various schemes and is consistent with this quasi-steady picture.

The results for the more difficult case in which the fluctuation frequency is high, $\Omega = 100$, and the time-step is small with 1000 points per time period are presented in Figure 7. For the flux difference scheme with steady preconditioning, the pressure response becomes very unstable and the amplitude overshoots the exact solution for velocity and pressure as seen in Figure 7(a) and Figure 7(b), respectively.

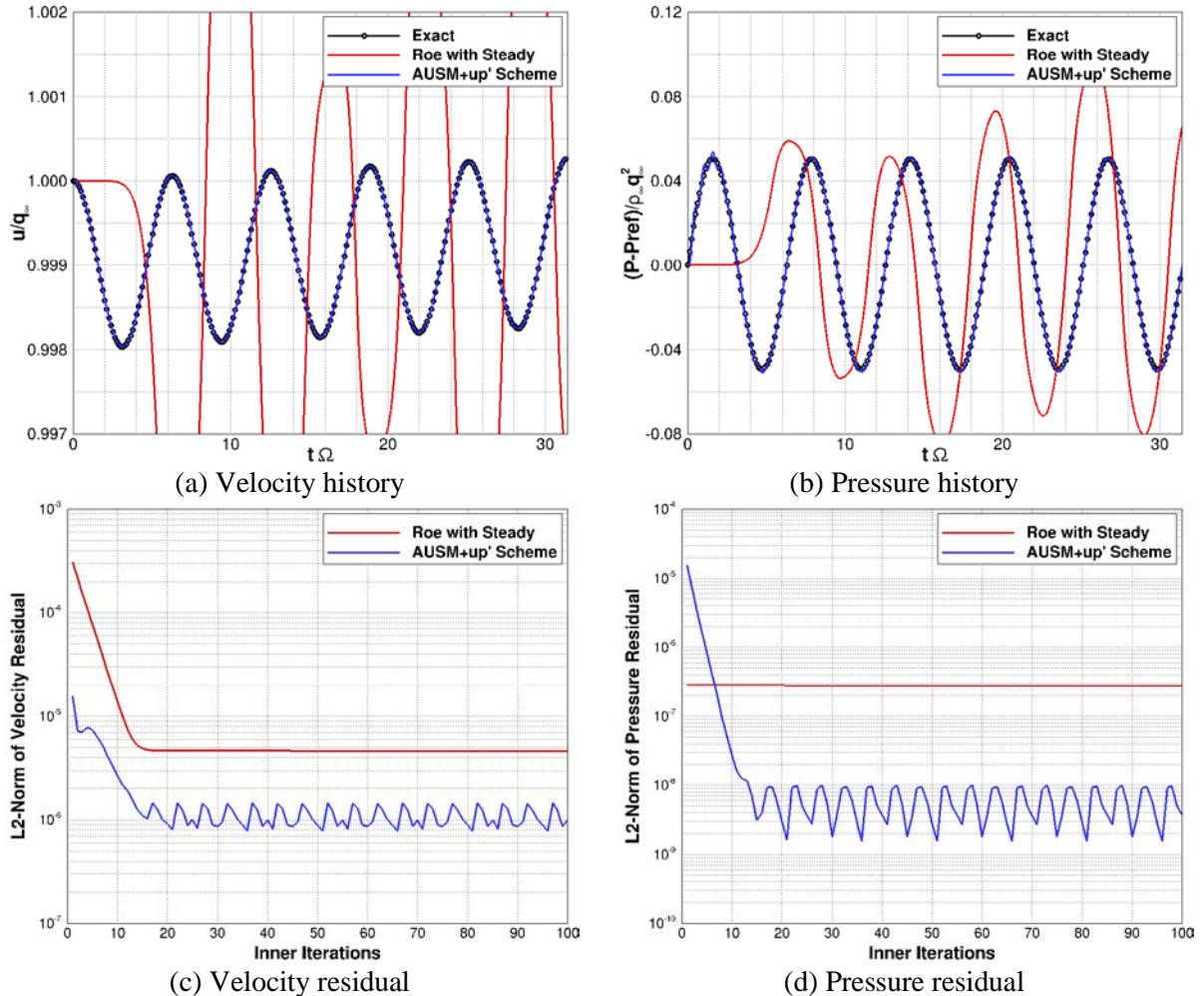


Figure 7: Velocity and pressure history and residuals for a high oscillation frequency ($\Omega = 100$) computed with a small time step (1000 PPW)

Moreover, an excessive phase error is also evident. The pressure residual for the steady preconditioning scheme is shown in Figure 7(d) and shows no convergence during the inner iterations. This is consistent with the incorrect flow results. The solutions computed using the blended flux difference scheme, and the AUSM+up' gave essentially the same results that matched the exact solution very well. Therefore, only the solution profiles predicted by the modified AUSM+up' scheme are shown in Figure 7. The velocity profile matches the exact solution perfectly. However, an initial fluctuation around the exact solution can be seen for the pressure transient in Figure 7(b). This fluctuation decays very quickly and the source of the error is not clear at this point. The convergence history plotted in Figure 7(c) and Figure 7(d) for the velocity and pressure residuals show that the AUSM+up' show good convergence slopes in general for both the velocity and pressure residual. In contrast the steady preconditioning shows very poor convergence consistent with the fact that steady preconditioning is inappropriate for high frequency pressure fluctuations. These results confirm that for low Mach number acoustic problems that the dissipation for the continuity equation (pressure variable) for both the AUSM+up' and the blended flux difference form must be consistent with the unsteady preconditioning form.

3.6 Simulations of Shock Tube with Small Pressure Difference

The final test case is a pure acoustic problem with low velocities. Here we model a shock tube with a very small pressure difference across the diaphragm that generates a low Mach number flow. In this particular case, a tube of length 1 m was chosen and the diaphragm was placed at $x = 0.5$. The

pressure on the left side of the diaphragm is initialized to 100028.04 Pa and the pressure on the right side is initialized to 100000 Pa; therefore the pressure difference is 28.04 Pa. The temperature is initialized to 300 K on both sides and the initial velocity is zero. A very weak acoustic waves results and generates a low Mach number flow of the order of 0.0001 in the contact interface.

In the calculations presented here, the time step was kept constant at 10 μ s and the calculations were done for a total time of 750 μ s. One-hundred inner iterations were used at each time-step and the unsteady Mach number for unsteady preconditioning was set to 1.0. The results of the previous problem confirmed that dissipation corresponding to unsteady preconditioning must be employed when simulating low Mach number acoustic problems. Therefore, the flux difference procedure with steady preconditioning will not be considered here.

Figure 8 shows the solution predicted using the baseline flux difference scheme with unsteady preconditioning and the blended flux difference procedure. Recall that the blended scheme uses unsteady preconditioning for the pressure waves and steady preconditioning for the velocity and temperature equation. For the solution profiles shown in Figure 8, the steady preconditioning parameter is set to $M_s = 0.01$ and the unsteady Mach number scale was set to $M_u = 1.0$. It can be seen in Figure 8(a) and Figure 8(b) that the acoustic wave and the contact interface have propagated to the correction location and the inner iteration convergence history shown in Figure 8(c) appears to be good for both flux difference procedures.

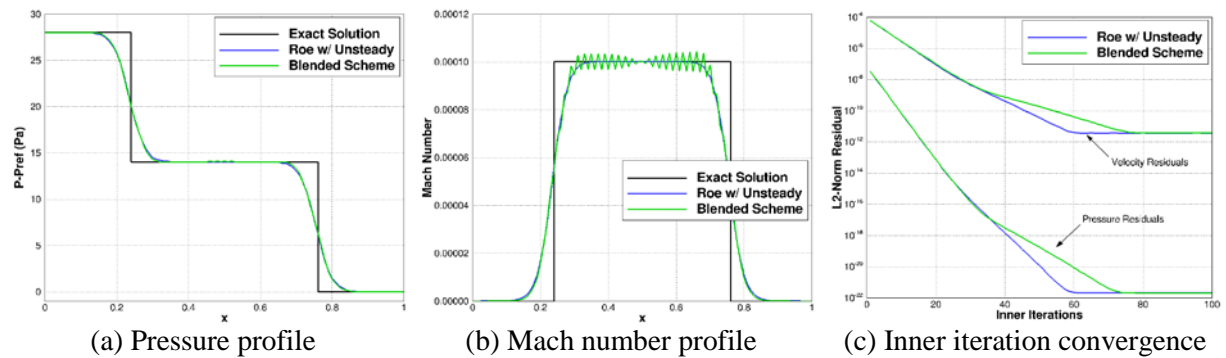


Figure 8: Shock tube solutions for the blended flux difference schemes with $M_u=1.0$ and $M_s=0.01$

However, closer inspection shows that the blended flux difference procedure produces small fluctuations in the pressure field at the contact interface which translates to substantial fluctuations in the velocity. The level of the fluctuations is sensitive to the disparity between the steady and unsteady preconditioning in the blending formula; the oscillation amplitude increases as the steady cut-off Mach number is reduced and the oscillation amplitude decreases as the steady cut-off Mach number is raised. If M_s is increased to 1.0 then the blended flux procedure is identical to the flux difference scheme with unsteady preconditioning which does not produce any oscillations.

The profiles predicted using the AUSM+*up* schemes are shown in Figure 9 for two different formulations. The profiles given by the blue-line include the modification to the mass flux dissipation term as given by Eqn. (25), however, does not include the modification to the pressure dissipation term as given by Eqn. (27). It can be observed from Figure 9 that this formulation produces fluctuations near the contact surface similar to what was seen from the blended flux difference procedure. Additional calculations were done with larger pressure ratios that increase the flow Mach number and it was found that the oscillations dissipate when the pressure difference is large enough to generate a Mach number of the order of 0.1 at the contact interface. This provides conclusive evidence that this numerical instability is related to acoustic propagation at low Mach numbers. In particular, these oscillations appear to be a fundamental manifestation of inadequate dissipation in the pressure flux that arises for low Mach number flows where the velocity arises from the propagating pressure pulse and appear for both blended flux difference and AUSM family of schemes.

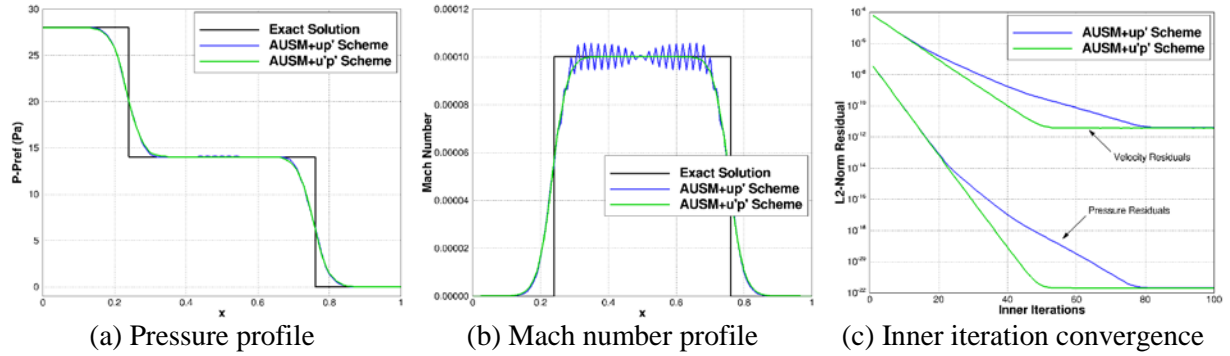


Figure 9: Shock tube solutions for the AUSM+up schemes with $M_u=1.0$

The derivation of the additional pressure dissipation in Eqn. (27) was in fact motivated by this test case which pointed out the inadequacy of the pressure dissipation term in both flux differenced and AUSM schemes. The velocity dissipation term in the pressure flux for the AUSM+up formulation goes to zero as the Mach number becomes low. However this dissipation may be required for reducing the pressure fluctuations for low Mach number acoustic waves and, therefore, the unsteady Mach number parameter was included in Eqn. (27) for the definition of f_a . In this so-called AUSM+u'p' scheme, the addition of the unsteady Mach number scale in the velocity dissipation term means that it retains a substantial value for unsteady low Mach number flows. The effect of this dissipation is illustrated in Figure 9 as indicated by the profiles given by the green line. The addition of the velocity dissipation allows for solutions that are smooth in both the pressure and Mach number profiles. Furthermore, the convergence is slightly improved and, therefore, provides a scheme that works in an accurate and efficient manner.

In summary, simulations for low Mach number shock tube configurations which represent a pure acoustic wave propagation that generates a very low Mach number flow indicates that both blended flux difference and the original AUSM+up/SLAU schemes have some fundamental deficiencies. While the location of the acoustic front was accurately captured, the pressure and velocity in the contact interface showed fluctuations that were a function of the local Mach number. For very weak acoustic waves where the flow Mach number was 0.0001 substantial oscillations were observed which dissipated as the Mach number rose to 0.1 (for a larger initial pressure difference). The fundamental deficiency in the dissipation was rectified in the AUSM+u'p' scheme by adding a pressure dissipation that is enforced only for unsteady low Mach number flows and represents a fundamental advancement to the AUSM family of schemes. Unfortunately for blended flux difference schemes there is no clear remedy apart from going to a pure unsteady preconditioning procedure (i.e. no blending) which obviously is not acceptable for the broader class of unsteady low Mach number flows that were tested.

4 Concluding Remarks

A generalized preconditioning framework that is both accurate and efficient for unsteady low Mach number flows is presented. It rectifies the deficiencies of standard steady/unsteady preconditioned flux difference schemes for simulating unsteady low Mach number flows and has been shown to apply to a broad class of problem encompassing both hydrodynamic and acoustic driven unsteady flows. Two classes of schemes were considered: flux difference schemes with blended steady and unsteady preconditioning and AUSM family of flux-splitting schemes. For flux difference schemes, generalized “blending” methodologies were developed (extending earlier work by Potsdam *et al.* [1]) wherein “unsteady” preconditioning is used for the pressure wave propagation, while “steady” preconditioning is used for the convected scalars that propagate at the fluid velocity. Two well-known AUSM schemes were analyzed initially; the AUSM+up by Liou [5] and the SLAU scheme by Shima and Kitamura [7][8]. The SLAU scheme was shown to be equivalent to the standard AUSM+ formulation (i.e., without the additional velocity and pressure dissipation proposed for low Mach

number flows). A more generalized formulation, the AUSM+ up ' scheme, that provides a unified framework for unsteady and steady flows using an unsteady Mach number parameter was developed; the unsteady Mach number parameter which can be specified as a local function of the flow physics is shown to provide the right selection of dissipation in the mass flux term. Furthermore a new velocity dissipation term was developed in the AUSM+ $u'p'$ formulation for acoustic flows to suppress spurious oscillations at very low Mach numbers.

Both the blended flux difference schemes and the modified AUSM+ up ' schemes were tested over a wide range of unsteady test cases that encompass both hydrodynamic and acoustic unsteadiness. Both schemes gave superior results with both the pressure wave and velocity propagation being captured accurately independent of time step and Strouhal number while providing adequate convergence for the inner iteration. However there were two notable exceptions: 1) for multi-dimensional flows such as the vortex propagation problem the blended flux difference schemes distorted the pressure field while the AUSM+ up ' scheme did not, and 2) for small pressure jump shock tube problem, oscillations in the contact surface were suppressed in the AUSM+ $u'p'$ scheme by the addition of a velocity dissipation term while no remedy was available for the blended flux difference procedure. Therefore, the modified AUSM+ up ' and AUSM+ $u'p'$ schemes are considered the superior scheme for unsteady low Mach number flows. We note here that the additional velocity dissipation term in AUSM+ $u'p'$ is needed only for suppressing the oscillations in the shock-tube problem. In all other cases, the modified AUSM+ up ' scheme proved to be the best choice. Resolving this discrepancy will be addressed in future work. Additionally, improvement of the inner iteration convergence for the AUSM+ up ' scheme also deserves further scrutiny. Here, the convergence may currently be hindered by the inconsistency between the LHS (implicit matrix) and RHS. Finally, future work will also focus on extending the methodology to frameworks that have both rotational and inertial frames as well as on developing generalizing the unsteady preconditioning parameter to consider local and global Strouhal numbers.

5 Acknowledgments

This work was performed under a Phase I SBIR funded by the U.S. Army under Contract No. W911W6-11-C-0039. Mr. Mark Potsdam was the contract monitor for this program and we gratefully acknowledge his support and technical guidance during the course of this effort.

6 References

- [1] Potsdam, M. A., Sankaran, V., and Pandya, S. A., "Unsteady Low Mach Preconditioning with Application to Rotorcraft Flows," Paper No. AIAA-2007-4473, 18th AIAA Computational Fluid Dynamics Conference, Miami, FL, 25-28 Jun 2007.
- [2] Venkateswaran, S., and Merkle C.L., "Analysis of Preconditioning Methods for the Euler and Navier Stokes Equation", VKI Lecture Series Monographs on Computational Fluid Dynamics, VKI LS 1999-03, von Karman Institute, March, 1999.
- [3] Turkel, E., "Preconditioning Techniques in Computational Fluid Dynamics", Annual Review of Fluid Mechanics, Vol. 31, pp. 385-416, 1999.
- [4] Briley, W.R., Taylor, L.K., and Whitfield, D.L., "High Resolution Viscous Flow Simulations at Arbitrary Mach Number", *Journal of Computational Physics*, 184(1), pp. 79-105, 2003.
- [5] Liou, M., "A Sequel to AUSM, Part II, AUSM+ up for All Speeds," *Journal of Computational Physics*, Vol. 214, No. 1, pp. 127-170, 2006.
- [6] Vigneron, D., Deliege, G., and Essers, J. A., "Crank-Nicholson Scheme for Solving Low Mach Number Unsteady Viscous Flows Using an Implicit Preconditioned Dual Time Stepping Technique" Fourth Int. Conference on Computational Fluid Dynamics, GHENT, BE, July 2006.

- [7] Shima, E, and Kitamura, K., "On New Simple Low-Dissipation Scheme of AUSM-Family for All Speeds," Paper No. AIAA-2009-0136, 47th AIAA Aerospace Sciences Meeting, Orlando FL, 5-8 Jan 2009.
- [8] Shima, E, and Kitamura, K., "CFD Method for Aero-Acoustics using all-speed numerical flux and preconditioned implicit time integration," 20th AIAA Computational Fluid Dynamics Conference, Honolulu, HI, 27-30 Jun 2011.
- [9] Sankaran, V., and Merkle, C.L., "Artificial Dissipation Control for Unsteady Computations", 16th AIAA Computational Fluid Dynamics Conference, Orlando, FL, AIAA 2003-3695, June 2003.
- [10] Sankaran, V., *et al.*, "CFD Simulations of Acoustic Wave Phenomena in Combustion Chambers," *Computational Fluid Dynamics 2004*, edited by C. Groth and D. W. Zingg, Proceedings of ICCFD3, Toronto, ON, 12-16 Jul 2004.
- [11] Roe, P., L., "Approximate Riemann solvers, parameter vectors, and difference schemes," *Journal of Computational Physics*, Vol. 43, 357-372, 1981.
- [12] Hosangad, A., Lee, R. A., York, B. J., Sinha, N., and Dash, S. M., "Upwind Unstructured Scheme for Three-Dimensional Combusting Flows," *Journal of Propulsion and Power*, Vol. 12, No. 3, pp. 494-503, May-June, 1996.
- [13] Hosangad, A., Lee, R. A., Cavallo, P. A., Sinha, N., and York, B. J., "Hybrid, Viscous, Unstructured Mesh Solver for Propulsive Applications," AIAA-98-3153, 34th AIAA/ASME/SAE/ASEE Joint Propulsion Conference and Exhibit, Cleveland, OH, July 13-15, 1998.
- [14] Hosangad, A., Cavallo, P. A., Arunajatesan, S., Ungewitter, R., and Lee, R. A., "Aero-Propulsive Jet Interaction Simulations Using Hybrid Unstructured Meshes," AIAA-99-2219, 35th AIAA/ASME/SAE/ASEE Joint Propulsion Conference and Exhibit, Los Angeles, CA, June 20-24, 1999.
- [15] Hosangadi, A., Ahuja, V., and Ungewitter, R.J., "Simulations of Rotational Cavitation Instabilities in the SSME Low Pressure Fuel Pump," AIAA-2007-5536, 43rd AIAA/ASME/SAE/ASEE Joint Propulsion Conf. & Exhibit, Cincinnati, OH, July 8-11, 2007.